Appl Microbiol Biotechnol (2017) 101:6551–6561
DOI 10.1007/s00253-017-8372-8

ENVIRONMENTAL BIOTECHNOLOGY

Modulation of calcium carbonate precipitation by exopolysaccharide in *Bacillus* sp. JH7

Hyun Jung Kim[1] · **Bora Shin**[1] · **Yun Suk Lee**[1] · **Woojun Park**[1]

Received: 8 February 2017 / Revised: 24 May 2017 / Accepted: 25 May 2017 / Published online: 22 June 2017

Abstract Extracellular polymeric substance (EPS) is proposed to facilitate calcium ion supersaturation through its nucleation effect during the microbially induced calcium carbonate precipitation (MICP) process. However, the supersaturation effect of Ca^{2+} via EPS in MICP has not been clearly demonstrated. Enhanced exopolysaccharide production of the alkali- and halotolerant MICP-capable bacteria, *Bacillus* sp. JH7, was achieved through glycerol addition. This was demonstrated by measuring cellular precipitation and Congo red binding. Interestingly, field emission scanning electron microscopy and energy-dispersive X-ray spectrometry analysis demonstrated that there was no MICP under glycerol-amended conditions. Although glycerol promoted exopolysaccharide capture of Ca^{2+} ions, Ca^{2+} embedded onto EPS did not participate in MICP formation. The pH was reduced in glycerol-added media, which led us to analyze high acetate production under our test conditions. Purified glycerol-induced exopolysaccharide showed a higher capacity of Ca^{2+} capture than the control. Quantitative RT-PCR analysis showed that three genes involved in exopolysaccharide production were highly upregulated by glycerol. The amounts of three detected monosaccharides (arabinose, glucose, and mannose) were altered by glycerol. Cell hydrophobicity measurements indicated that glycerol could confer more hydrophilic characteristics to cells, which might enhance Ca^{2+} binding onto EPS. Unexpectedly, our data demonstrated, for the first time, that glycerol could promote exopolysaccharide and acetate production under our test condition, which could inhibit MICP by reducing the availability of free Ca^{2+}.

Keywords Calcium carbonate · *Bacillus* · Exopolysaccharide · Glycerol

✉ Woojun Park
wpark@korea.ac.kr

[1] Laboratory of Molecular Environmental Microbiology, Department of Environmental Science and Ecological Engineering, Korea University, Seoul 02841, Republic of Korea

Introduction

Microbially induced calcium carbonate precipitation (MICP) is an established process that commonly occurs in a variety of natural environments, including soils, caves, hot springs, freshwater, and hypersaline, by incorporating a significant amount of atmospheric CO_2 through the biogenic activity of living microorganisms (Gat et al. 2016; Kim et al. 2016; Zhu and Dittrich 2016). Carbon immobilization in carbonates is reportedly carried out by photosynthetic bacteria such as *Cyanobacteria*, denitrifying *Bacillus*, ureolytic *Pseudomonas*, *Acinetobacter*, *Myxococcus*, *Bacillus* (*Bacillus cohnii*, *Bacillus megaterium*, *Bacillus subtilis*, *Bacillus cereus*, *Bacillus sphaericus*), *Sporosarcina* (*Sporosarcina pasteurii*, *Sporosarcina soli*, *Sporosarcina ureae*), and sulfur-oxidizing *Arthrobacter* (Jansson and Northen 2010; Erşan et al. 2015; Kim et al. 2016; Kumari et al. 2016; Zhu and Dittrich 2016). These bacteria promote the alkaline pH of the surrounding area that readily accelerates the deposition of intracellular/extracellular calcium carbonate (Zamarreño et al. 2009; De Muynck et al. 2010; Couradeau et al. 2012). This carbonate deposition process is nowadays acknowledged for its potential for the stabilization of soils, self-healing concrete, and carbon sequestration in reducing global warming (De Muynck et al. 2010; Gat et al. 2016; Kumari et al. 2016; Zhu and Dittrich 2016).

Bacterial extracellular polymeric substances (EPS) consisting of proteins, nucleic acids, lipids, and exopolysaccharides are reissued factors in microbial MICP, and might be linked to provide surfaces

for the supersaturation of calcium ions (Dupraz et al. 2009; Tourney et al. 2009; Santana and Gonzalez 2015; Zhu and Dittrich 2016). Traditionally, EPS is known to function as protective templates for maintaining bacterial viability in various forms of slime or microcapsular polysaccharides (De Philippis et al. 2011; Nwodo et al. 2012; Jittawuttipoka et al. 2013). However, adherent properties of bacterial EPS began to be acknowledged for providing nucleation site during MICP, owing to diverse properties in composition and function of EPS (Ercole et al. 2007; Nwodo et al. 2012; Zivkovic et al. 2015) such as heteropolysaccharide consisting of high-molecular-mass residues such as glucose, galactose, mannose, arabinose, and fructose (Pereira et al. 2009; Chowdhury et al. 2011; Kumar and Shah 2015; Zivkovic et al. 2015), as well as negatively charged residues of carboxyl, phosphate, amine, and hydroxyl groups (Braissant et al. 2007; Oggerin et al. 2013). Because of their viscous and negatively charged characteristics, EPS can incorporate nearby metal cations such as Mg^{2+}, Fe^{3+}, Mn^{2+}, and Ca^{2+}, and induce encrustation of microbially mediated extracellular calcium carbonate (Shao et al. 2014; Zhu and Dittrich 2016), thereby, accelerating aggregation of bacteria and calcium carbonate (Zhu and Dittrich 2016). Oxygen concentration, pH level, temperature, media composition, and salt ion concentration affect the composition and amount of EPS (Oggerin et al. 2013; Shao et al. 2014), which differentiates the morphology and mineralogy of those induced by bacterial species (Ercole et al. 2007; Zhu and Dittrich 2016). Regarding how bacteria adapt to different environments, the chemical characteristics of the bacterial surface involving EPS vary between the exposed environments, which significantly alters the morphology of precipitated calcium carbonate.

Despite the overall potential of EPS inducing bacterial MICP, EPS can act as a duplex inhibitor in microbial MICP (Dupraz et al. 2009; Zhu and Dittrich 2016). It can remove free Ca^{2+} from reacting to carbonates or bicarbonates by binding them to negatively charged groups composing of EPS, thus reducing the possibility of supersaturation of Ca^{2+} ions around the cell wall and precipitation of calcium carbonate (Zhu and Dittrich 2016). Therefore, excessive amounts of EPS can reduce the potential of microbial MICP. However, despite of a possible link between EPS' nucleation site and MICP (Dupraz et al. 2009; Tourney et al. 2009), to this date, there have been relatively few reports demonstrating a direct correlation between EPS and MICP (Bai et al. 2017).

In this study, we investigated how glycerol-induced exopolysaccharide of EPS modulates microbial MICP in *Bacillus* sp. JH7, the MICP-capable bacteria isolated from old concrete wall (Kim et al. 2016). We investigated whether excessive amounts of exopolysaccharide under glycerol-amended conditions could induce a reduction in the microbial MICP of strain JH7 by reducing the concentration of free Ca^{2+} participating in MICP as a result of the tight bonding connection between EPS and Ca^{2+}. A significant drop in pH due to high acetate production through glycerol metabolism, alteration of exopolysaccharide composition, cell hydrophobicity, and motility were evaluated to elucidate the inhibitory effect of MICP by glycerol.

Materials and methods

Bacterial strain and growth conditions

Bacillus sp. JH7 was isolated from the inner part of the concrete wall of an old building (Kim et al. 2016). The genome of strain JH7 was sequenced as scaffolds as previously described (Park et al. 2016). Its sequence and annotation information can be accessed from the National Center for Biotechnology Information (NCBI) database under the accession numbers, LPUS00000000 and KU168426, respectively. Also, strain JH7 was deposited in Korean Agricultural Culture Collection (KACC) under the number KACC 19226. Strain JH7 was incubated in Luria-Bertani (LB) broth at 37 °C overnight, prior to experiments. The media used for the experiments consist of 0.1% (*g*/*v*) yeast extract, 1% (*g*/*v*) NH_4Cl, 0.2% (*g*/*v*) $NaHCO_3$, 0.3 M urea, and 25 mM $CaCl_2$ (YUC media). The following were added if necessary: 0.3% (*v*/*v*) glycerol (YUCG; YUC with glycerol), glucose, galactose, fructose, xylose, sorbitol, and raffinose.

Quantification of precipitates and exopolysaccharide

Strain JH7 was aerobically incubated in YUC, supplemented with 0.3% (*g*/*v* or *v*/*v*) glucose, galactose, fructose, xylose, sorbitol, raffinose, and glycerol, if needed, for 72 h (37 °C, 220×*g*). The cells were centrifuged (20 min, 3000×*g*) to precipitate the cell-calcium carbonate aggregated pellet, freeze-dried, and measured in dry mass. Exopolysaccharide quantification was conducted according to a previous study (Kim et al. 2016). One milliliter of cell culture was incubated at 37 °C for 30 min with Congo red (CR) at a final concentration of 35 mg/l. After centrifugation (10 min, 13,000×*g*), the supernatant was measured at OD_{480} and calculated using the obtained standard curve equation. The measurement value was normalized to OD_{600} of 1 ml of cell culture.

FE-SEM, EDX, and XRD analysis and mineral purification

For microbially induced MICP analysis, strain JH7 was incubated in YUC and YUCG for 72 h. Then, 5 ml of cells was harvested by centrifugation (1 min, 13,000×*g*), and the pellets were fixed using Karnovsky's fixation method at 4 °C overnight. After cold incubation, the pellets were washed with 0.05 M potassium phosphate buffer three times for 10 min each at 4 °C. Dehydration of cells was performed at room temperature using 100% ethanol. The samples were coated

with platinum (Pt) before field emission scanning electron microscopy (FE-SEM) (FEI, Japan) analysis. Energy-dispersive X-ray (EDX) spectrometry mapping analysis was conducted using the NORAN System 7: Silicon Drift Detector (Thermo Fisher Scientific, USA), with an accelerating voltage of 15 kV.

To observe sole minerals induced by strain JH7, the culture was boiled for up to 1 h to lyse the bacteria and then filtered using nitrocellulose membrane filters, pore size 0.45 μm (Whatman, England), to obtain mineral. Minerals were completely air-dried before EDX analysis. To determine whether precipitates are $CaCO_3$, X-ray diffractometer (XRD; Dmax2500/PC) (Rigaku, Japan) analysis was conducted. The culture was freeze-dried prior to experiment.

HPLC analysis for metabolite analysis

Strain JH7 (5 ml) was incubated in YUCG medium for 72 h and then centrifuged (1 min, 13,000×*g*) to obtain a clear supernatant for the analysis of acidic metabolites by UV/visible high-performance liquid chromatography (HPLC) (1525, 2707, 2489, 2414, CHM, Waters Co., USA). The method was conducted according to the manufacturer's instructions. Briefly, the type of column used was Aminex HPX-87H (Bio-Rad, USA), which was set to 30 °C. H_2SO_4 (5 mM) was used as the solvent, and the flow rate was fixed to 0.6 ml/min. HPLC analysis was performed by Biosystems, Korea.

Exopolysaccharide purification and calcium ion quantification

Exopolysaccharide purification was conducted using the ethanol precipitation method. Strain JH7 was incubated in 1 l of YUC and YUCG media for 72 h, and was centrifuged to obtain a clear supernatant. Three times the volume of the ethanol supernatant was added and incubated at 4 °C overnight. Then, the sample was centrifuged, and the pellets were washed three times with 80% ethanol solution, followed by three washes with PBS to remove residues, and then freeze-dried. To analyze the efficiency of exopolysaccharide of EPS capturing calcium ions, the remaining calcium ion concentration was examined using a calcium ion-selective electrode (ISE; Thermo Fisher Scientific, USA). All samples were centrifuged to obtain a clear supernatant prior to ISE analysis.

Expression levels of genes involved in an exopolysaccharide operon by qRT-PCR

For qRT-PCR, total RNA was isolated from 50 ml of cells at stationary phase using the RNeasy Mini Kit (Qiagen), according to the manufacturer's instructions. Complementary DNA (cDNA) was synthesized from 1 μg of RNA, and the primer pairs (AU379_RS18510 F/R (F_GCTCGTGACATTGCTAACAC A, R_ TTGGGCGTGGTTTAATTGGC), AU379_RS18535 F/R (F_ ATGGGGGCTCATGTAAAGGC, R_ AGCCTCAA TGACTTCGCTCA), and AU379_RS18550 F/R(F_ TGCTTTAGGGGAACAGTGGA, R_ TCGGGATC ATCGGATACCTGT)) were synthesized using RevertAid H Minus First Strand cDNA Synthesis Kit (Fermentas). Then, qRT-PCR was conducted using StepOnePlus (Thermo Fisher, USA). For real-time RT-PCR, the same RNA sample was used to produce cDNA. cDNA (1 μl), 5 pmol of primers, 0.5× SYBR Green, and 1 unit of Taq polymerase (Fermentas) were also used. Fluorescence was measured at each endpoint of extension at 72 °C, and was analyzed using the StepOne software (Thermo Fisher, USA). The 16S ribosomal RNA (rRNA) gene was used for quantification.

HPAEC analysis

The purified exopolysaccharide of strain JH7 incubated in YUC and YUCG for 72 h was freeze-dried prior to EPS composition analysis via High-Performance Anion-Exchange Chromatography (HPAEC; ICS-5000, Dionex Co., USA). The CarboPac PA-1 (Dionex Co., USA) column was used with 18 mM NaOH as the solvent, at a flow rate of 1.0 ml/min at 25 °C. HPAEC was performed by Biosystems, Korea.

Salt aggregation test and microbial adhesion to hydrocarbon assay

Bacteria (10^8 cell/ml) from YUC and YUCG were suspended in 0.001 M sodium phosphate buffer (pH 6.8). Ten microliters of bacterial suspension was dotted onto sterile glass slides and immediately mixed with an equal volume of ammonium sulfate at concentrations from 0.2 to 4 M. Safranin (1 μl) was also added to the mixture for easy aggregation recognition. Strain JH7 inoculated in YUC and YUCG was suspended with PBS to obtain OD_{600} = 0.5. Next, 3 ml of bacterial suspension was vigorously vortexed with filtered hexadecane (100, 150, 200, 250, and 300 μl) in a sterile glass tube for 1 min. Then, the tubes were stationed until a vivid layer of water-oil phase was visible. Bacteria from the water layer on the bottom were pipetted separately, and the OD_{600} was measured.

Colony motility assay

Strain JH7 (1 ml) that was incubated until stationary phase (15 h) was washed twice with PBS, prior to inoculating 10 μl of bacterial suspension onto YUC and YUCG agar plates. Continuous static incubation was held in 37 °C, and colony motility in the sample was monitored in a time-dependent manner using ColonyDoc-It™ (UVP, USA).

Results

Enhanced bacterial precipitation and exopolysaccharide production by glycerol

To maximize biological MICP via bacteria and minimize its chemical synthesis, MICP medium was optimized by testing several concentrations of nutrients and $NaHCO_3$ because these two parameters could affect chemical MICP. Since the amount of calcium ion dissolved in the media was equivalent in all conditions, the remaining calcium ion concentration of the media (1% NH_4Cl, 0.3 M urea, 25 mM $CaCl_2$) was analyzed in media without bacteria. Several concentrations of yeast extract (YE) (0.1 to 0.3%) and $NaHCO_3$ (0.2 to 3.2%) were tested, and the concentration of remaining calcium ion was monitored using calcium ion-selective electrode (ISE). Low concentrations of YE (0.1%) and $NaHCO_3$ (0.2%) were chosen for observing biological MICP because of their minimal effect on chemically synthesized calcium carbonate precipitation under our tested conditions (Fig. 1a, b). To gain insight into possible MICP efficiency through enhanced EPS production in *Bacillus* sp. JH7, 0.3% of several different carbon sources including glucose, galactose, fructose, xylose, sorbitol, raffinose, and glycerol were supplemented in YUC medium, and the amount of precipitates and exopolysaccharide produced by strain JH7 was measured (Fig. 1c, d). Although there was no direct quantitative correlation between precipitates and exopolysaccharide production, the precipitated mass and exopolysaccharide were much higher under the additional carbon source conditions (Fig. 1c, d). The supplementation of glycerol to the media induced the production of precipitate biomass by 3-fold and EPS production by 4.4-fold. Therefore, glycerol was chosen for further examination as it demonstrated the most enhanced production of precipitates and exopolysaccharide.

Inhibition of calcium carbonate precipitation by glycerol

To verify whether the biomass precipitates in glycerol-amended media (YUCG) have calcium carbonate minerals, precipitates from control (YUC) and YUCG were analyzed using field emission scanning electron microscopy (FE-SEM) and energy-dispersive X-ray (EDX). Strain JH7 was capable of inducing extracellular MICP in YUC in form of $CaCO_3$, as the aggregated minerals were determined as calcium ions and $CaCO_3$ by EDX and XRD analysis, respectively (Fig. 2). The induced calcium carbonates in YUC had amorphous rough surfaces with some of the mineral particles set on top of the bacterial surface, representing the nucleation effect. However, most of them seemed to precipitate away from the cell surface and then aggregate to each other, indicating possible induction of a specific micro-atmosphere for bacterial MICP. Conversely, strain JH7 was unable to precipitate calcium carbonate under glycerol conditions, as neither calcium ion nor minerals of calcium carbonate were detected via EDX and XRD, respectively (Fig. 2c, d). Rather, the cells showed elongated rod shapes bound with mucous EPS, and the extent of aggregation was more severe than YUC as the aggregates looked like supercoiled springs (Fig. 2a). Our data suggests that glycerol-induced exopolysaccharide could be inhibitory to MICP.

Glycerol-induced physiological changes: growth, Ca^{2+} absorption, pH, and metabolites

To understand why glycerol addition inhibited precipitation of calcium carbonate minerals in strain JH7 despite the highest production of exopolysaccharide, the growth measurement, ionized calcium concentration, pH changes, and metabolites were monitored. Improved growth of strain JH7 was observed 8 h after inoculation only in YUCG, probably because of initiation of glycerol consumption, depicting a diauxic growth curve (Fig. 3a). The maximum OD_{600} under the glycerol condition was approximately 2-fold higher than the control media until 48 and 72 h. After 72 h, the OD_{600} values of strain JH7 in both media decreased, most likely due to depletion or limited accession of nutrients because of the encrustation effect of induced MICP. Strain JH7 incubated in both YUC and YUCG was capable of capturing free Ca^{2+}, and the consumption pattern was similar. The remaining Ca^{2+} concentration in both YUC and YUCG drastically decreased after 4 h of incubation (Fig. 3a), and a sharp decrease in Ca^{2+} concentration occurred at 4 h in YUCG media. At 96 h, the remaining ionized calcium was almost zero, which suggested that Ca^{2+} was either precipitated as $CaCO_3$ or simply absorbed onto EPS produced by strain JH7. Based on our previous FE-SEM and EDX data (Fig. 2), it appears that overproduced exopolysaccharides by glycerol addition could absorb Ca^{2+}, thus inhibiting strain JH7 to precipitate calcium carbonate. Interestingly, the pH of YUC increased from 7.325 to 8.32 at maximum, while in YUCG, the pH decreased from 7.31 to 4.635 (Fig. 3a). These pH differences started only after 8 h of incubation, indicating that the reduced pH could further inhibit MICP due to the alkali pH requirement for MICP formation. To delineate the types of metabolites during glycerol metabolism which induced acidity in YUCG, higher-performance liquid chromatography (HPLC) was conducted using the supernatant of YUCG. High concentration of acetic acid and low amounts of pyruvic acid were detected at the concentration of 23.9 and 0.56 mg/l, respectively (Fig. 3b). Other acidic metabolites such as succinic, formic, levulinic, propionic, glucuronic, glycolic, lactic, citric, malic, and oxalic acids were not observed.

Absorption capacity of purified exopolysaccharide

To determine the modulation effect of glycerol-induced exopolysaccharide, the Ca^{2+} binding capacities of purified exopolysaccharide from YUC and YUCG media were analyzed using ISE. Purified exopolysaccharide extracted from cells grown

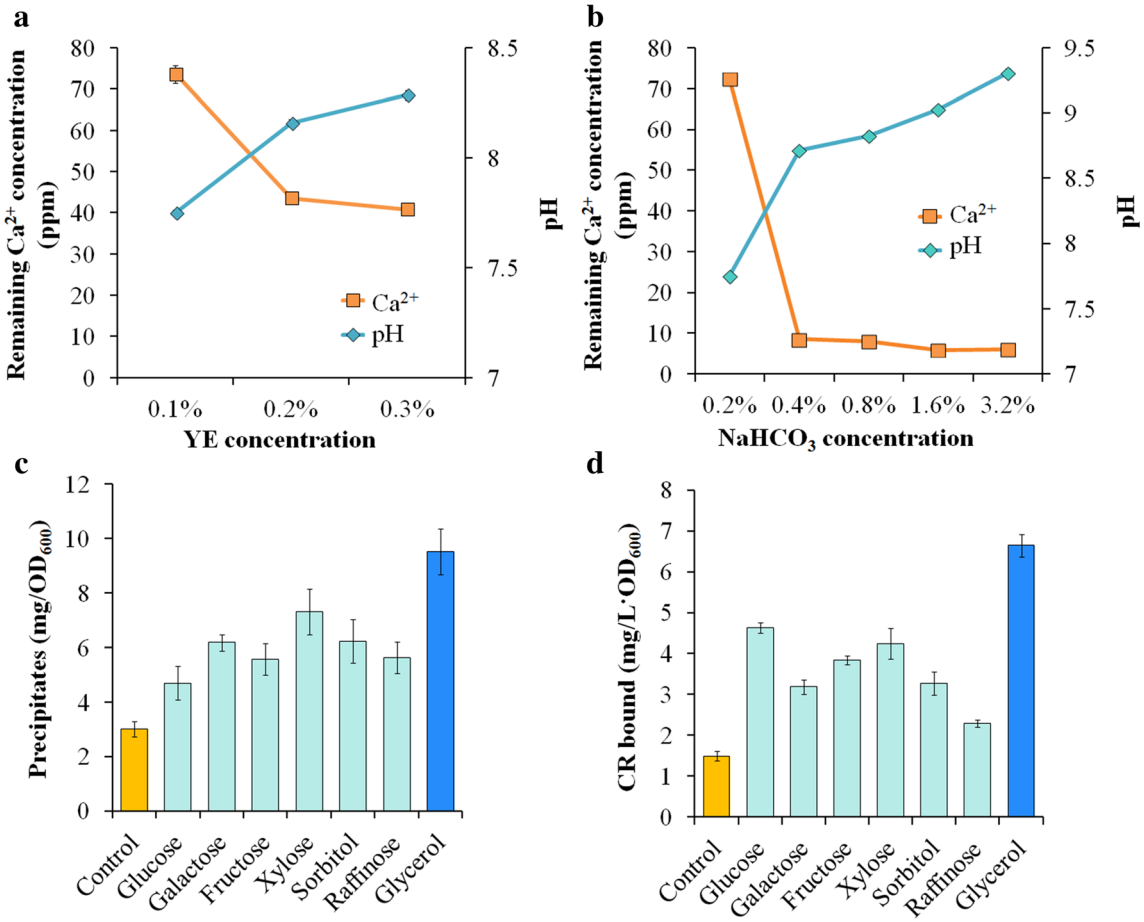

Fig. 1 Optimization of calcium carbonate precipitation inducing media and quantification of precipitates (cell biomass and putative calcium carbonate mineral mass) and exopolysaccharide. **a** ISE and pH analysis in YE concentration gradient. **b** ISE and pH analysis in $NaHCO_3$ concentration gradient. **c** Quantification of precipitates. **d** Quantification of EPS using Congo red

in both YUC and YUCG media demonstrated the capacity to bind to Ca^{2+} cation, since the concentration level of Ca^{2+} was reduced in both conditions. However, the exopolysaccharide extracted from cells grown in YUCG showed higher binding efficiency of Ca^{2+} than that of YUC-grown cells (Fig. 4a). The partial genome of strain JH7 was previously sequenced (Park et al. 2016), and the putative exopolysaccharide operon-forming genes of strain JH7 were determined by comparison with exopolysaccharide-encoding genes from the genomes of *B. cereus* and *Bacillus thuringiensis* groups. Among 17 exopolysaccharide candidate genes, three genes (AU379_RS18510; capsular biosynthesis protein, AU379_RS18535; UDP-glucose 6-dehydrogenase, AU379_RS18550; glycosyl transferase) were chosen to examine relative gene expression under YUC and YUCG media because the glycerol-supplemented condition induced a higher amount of exopolysaccharide as shown in our experiments. The expression of genes involved in exopolysaccharide synthesis was distinctively higher under YUCG conditions (Fig. 4b), which is consistent with the mass of purified exopolysaccharide from both media (Fig. 4c).

Change of exopolysaccharide composition and cell membrane hydrophobicity under glycerol

To validate whether glycerol alters the chemistry of the cell membrane, exopolysaccharide composition was analyzed in comparison to YUC and YUCG, using HPAEC. Purified exopolysaccharide extracted from cells grown in both YUC and YUCG media consisted of arabinose, glucose, and mannose, whereas rhamnose, galactose, and xylose were not detected (Fig. 4d). The composition concentration pattern differed between exopolysaccharides from cells grown in YUC and YUCG. Among the three monosaccharides, exopolysaccharide from cells grown in YUCG had 2-fold more arabinose and glucose than exopolysaccharide of YUC. Mannose was detected the highest concentration in YUC media (25.9 μg/mg), whereas 19.6 μg/mg was identified in YUCG. The change in monosaccharide composition linked to membrane surface hydrophobicity is unclear; however, we speculated that these different monosaccharide compositions might contribute to cell surface hydrophobicity, which results

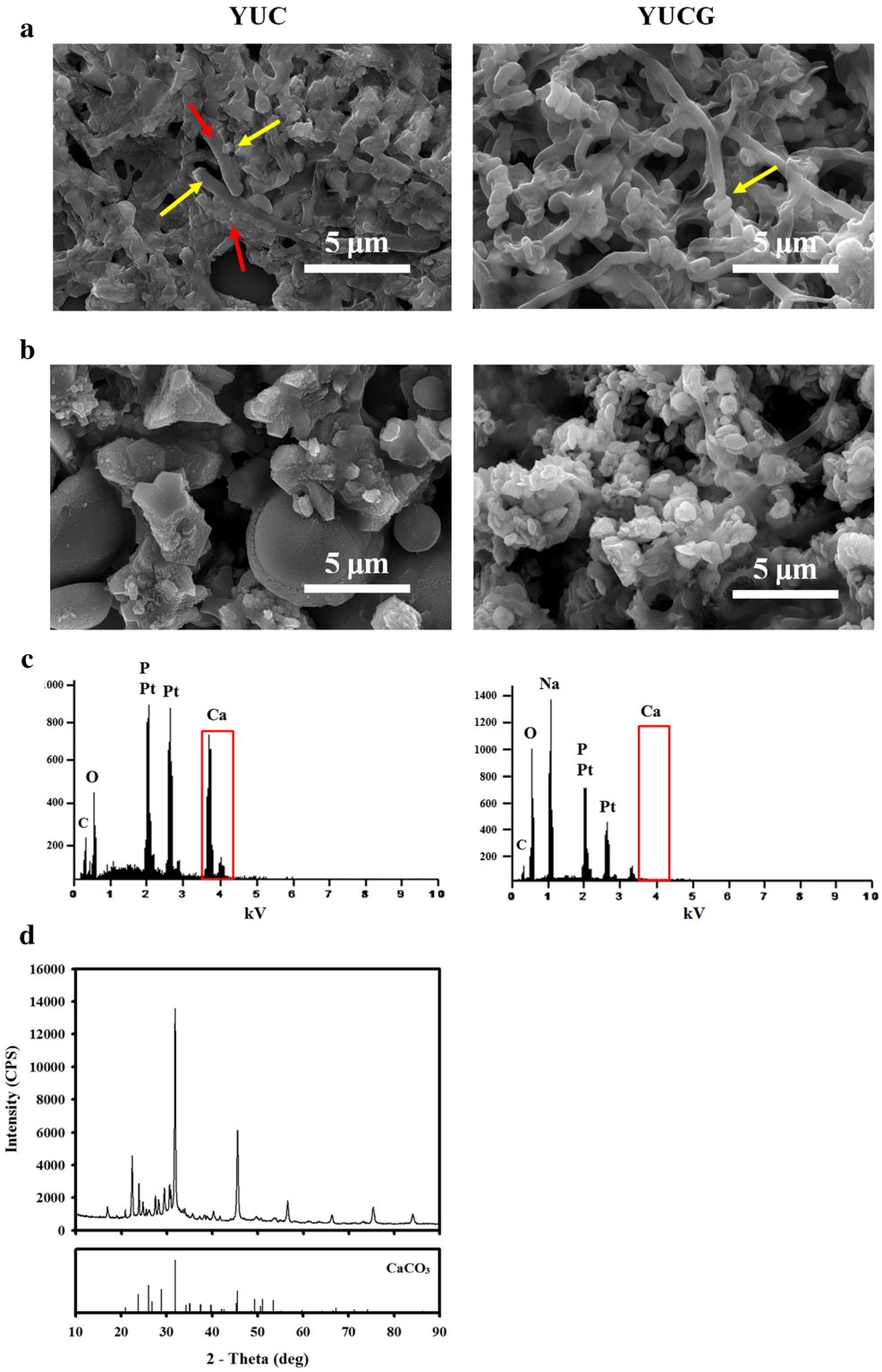

Fig. 2 FE-SEM/EDX/XRD analysis of precipitates from YUC and YUCG media. **a** FE-SEM analysis of bacterial precipitates of YUC and YUCG, 72 h after incubation. *Red arrows* indicate MICP, while *yellow ones* indicate the whole cell of strain JH7. Magnification was ×10,000, and the *scale bar* indicates 5 μm. **b** FE-SEM analysis of purified precipitates from YUC and YUCG media. **c** EDX of bacterial precipitates from YUC and YUCG. The *red box* indicates Ca^{2+} peaks. **d** XRD analysis of minerals precipitated in YUC medium. The mineral indicates $CaCO_3$, with 2-Theta (deg) indicating 31.873 (Color figure online)

in different Ca^{2+} absorption. The cell hydrophilicity of strain JH7 incubated in YUC and YUCG media was evaluated; the salt aggregation test (SAT) illustrates that the surface of strain JH7 incubated in YUCG became more hydrophilic than that of YUC, as a higher threshold was observed (YUCG 1.65 M NH_4Cl, YUC 1.025 M NH_4Cl) (Fig. 5a, b). This observation is consistent with microbial adhesion to hydrocarbon (MATH) test, which at 100 μl volume of hexadecane, the percentage of initial OD_{600} was higher in the YUCG condition, suggesting reduced attachability (hydrophobic) compared to strain JH7

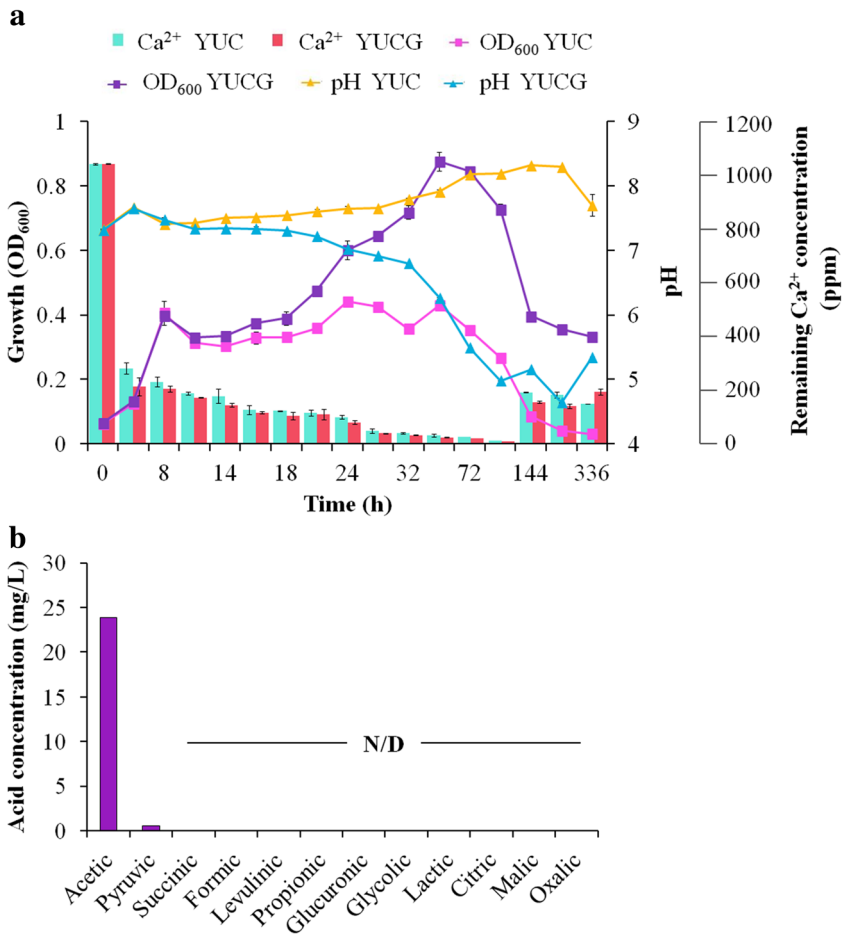

Fig. 3 Growth measurement of strain JH7 in YUC and YUCG media. **a** Time-wise measurement of growth in OD_{600}, pH, and ISE analysis of YUC and YUCG. **b** High-performance liquid chromatography (HPLC) analysis of organic acid metabolites of YUCG

incubated in YUC (Fig. 5c). Therefore, these hydrophilic changes might have affected the levels of free Ca^{2+} in participating MICP.

Reduced motility through calcium carbonate encrustation

To analyze the existence of a relatively differentiated regulation pattern of motility formation and exopolysaccharide production of strain JH7, a colony motility assay was performed in YUC and YUCG media. In YUC and YUCG, marked differences in phenotype were observed between the colonies developed by the initially congruent strain JH7 that was pre-incubated in LB, although the diameter of the colony formed was similar at each time point (Fig. 6). YUCG induced the formation of reasonably opaque white, smooth surfaces, whereas YUC colonies were a rather dense, opaque circled belt with no changes in size. Inside this circle, mineral looking colony dots were visible, which became a little vague as incubation time increased. Both conditions demonstrated radial shaped motility, but with opacity differences. Colony motility in YUC presented a semi-translucent phenotype, whereas YUCG was comparably turbid. In addition, the wrinkles of YUCG were more distinct and thick than YUC, which correlated with the growth difference between YUC and YUCG.

Discussion

The nucleation effect of bacterial EPS has also been an accepted notion for bacterial MICP (Dupraz et al. 2009; Tourney et al. 2009; Kim et al. 2016; Zhu and Dittrich 2016). However, only few in-depth studies on the scientific linkage between EPS and MICP have been scrutinized. In this study, the supersaturation of Ca^{2+} around the cell membrane, specifically nucleation of EPS, has been examined during bacterial MICP formation. The Ca^{2+} cation absorption efficiency of EPS under different media conditions was distinctive from each other, and the results show that excessive amount of exopolysaccharide production induced by glycerol could inhibit MICP formation probably because of a strong ionic bond between Ca^{2+} and exopolysaccharide.

Recent studies on microbial MICP use a variety of MICP inducing media such as urea-$CaCl_2$ (Kim et al. 2016), 0.3% beef extract, 0.5% peptone, 2% urea (Kang et al. 2014), 0.4% YE, 0.5% glucose, 1.5% calcium acetate (Park et al. 2013),

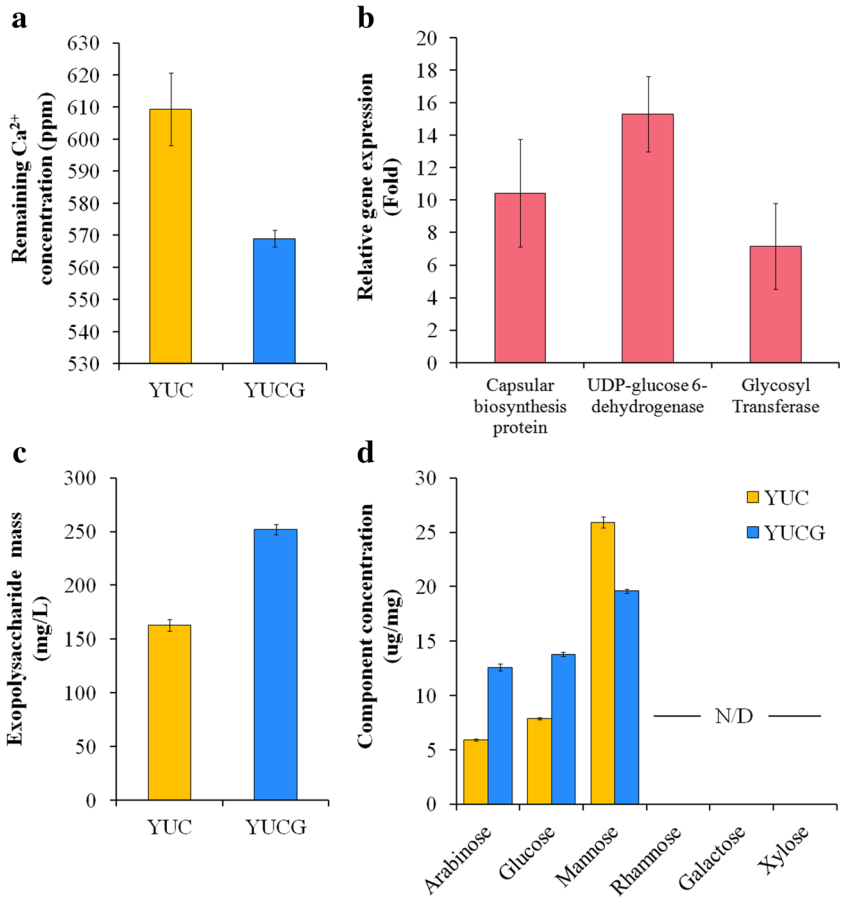

Fig. 4 Discrepancy in the chemical properties of purified exopolysaccharide under YUC and YUCG. **a** ISE analysis of the Ca^{2+} absorbing capability of the purified exopolysaccharide of YUC and YUCG. **b** Relative gene expression of three genes of the putative exopolysaccharide-related EPS operon of strain JH7. The values indicate gene expression under YUCG, which was normalized to gene expression under YUC. **c** Quantification of exopolysaccharide mass of YUC and YUCG using the EtOH precipitation method. **d** High-performance anion-exchange chromatography (HPAEC) analysis of the exopolysaccharide composition of YUC and YUCG

0.3% NB, 0.212% $NaHCO_3$, and 30 mM $CaCl_2$ (Hammes et al. 2003). However, these studies do not account for the fact that those media conditions not only help bacterial MICP, but also promote its chemical synthesis. Although NH_4Cl and $NaHCO_3$ could buffer the medium, $NaHCO_3$ can be a source for HCO_3^-, which could react with the Ca^{2+} of the given $CaCl_2$. In addition, nutrient sources such as nutrient broth can capture Ca^{2+} due to an ionic reaction of protein residues in the aqueous state. Therefore, minimizing the amount of possible reacting $NaHCO_3$ and nutrient ingredients is crucial. In this study, we utilized YE at a concentration of 0.1% (*g*/*v*) because YE has a lower amount of nutrients than Difco Nutrient Broth consisting of peptone beef extract, which promotes bacterial growth as carbon and nitrogen sources (Peighamy-Ashnaei et al. 2007). Furthermore, more than 3 g/l of YE can induce the inhibition of microbial MICP due to the prevention of electron exchange between Ca^{2+} and the anionic cell wall (Seifan et al. 2016). In addition, the combination of YE, urea, and calcium chloride is known to proliferate bacterial MICP in *Bacillus licheniformis*, which has 94.37% 16S rRNA sequence identity with strain JH7 (Seifan et al. 2016). Our results demonstrate that the lowest concentration of YE generated the least chemical synthesis of MICP (Fig. 1a); however, since YE itself showed capability of absorbing Ca^{2+}, urease activity was further investigated to determine whether sole YE had urease activity to decompose urea. Yet, no significant differences in urease activity in all YE concentration gradients were observed (data not shown). With respect to YE, $NaHCO_3$ also showed a high capability of chemical MICP, as the calcium carbonate saturation point seemed to be at 0.4% $NaHCO_3$ with no significant change of Ca^{2+} parts per million thereafter. This emphasizes the prompt chemical reaction of Ca^{2+} with HCO_3^-, which delineates that a higher amount of $NaHCO_3$ could reduce the amount of available Ca^{2+} sources for bacteria to use in microbial MICP.

The amount of precipitates (cell and MICP) is important in application, as it alters the efficiency of plugging and cementation effects (Zamarreño et al. 2009; De Muynck et al. 2010; Zhu and Dittrich 2016). Here, EPS can help absorb free calcium ions to precipitate calcium carbonate and aggregate cells and minerals together to form organic-inorganic monomers (Braissant et al. 2007; Baker et al. 2010; Rusznyák et al. 2012; Oggerin et al. 2013; Zhu and Dittrich 2016). Therefore, many scientists assume that the velocity and efficiency of microbial MICP can be increased under sufficient EPS production. To test this possibility, we attempted to increase the production of exopolysaccharide of strain JH7

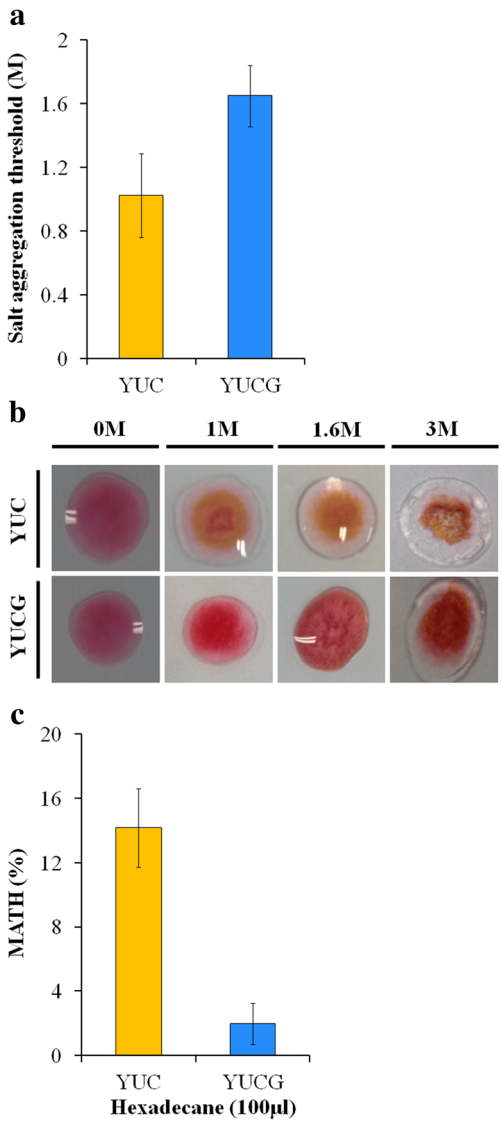

Fig. 5 Change in cell hydrophobicity of strain JH7 incubated in YUC and YUCG. **a** Salt aggregation test (SAT). **b** Visualization of SAT test using safranin red. **c** Microbial adhesion to hydrocarbon (MATH) test

using several monosaccharides (glucose, galactose, fructose, xylose, sorbitol, raffinose) and glycerol, which is composed of exopolysaccharides of *Bacillus* (Baker et al. 2010; Chowdhury et al. 2011; Zivkovic et al. 2015) and known to promote motility formation (Gallegos-Monterrosa et al. 2016). Strain JH7 produced the highest amount of exopolysaccharide under glycerol-amended conditions, which proliferated better growth; however, it was not able to induce bacterial MICP (Fig. 3). We assume the reason for this inhibition effect as a result of utilization of glycerol as a carbon source, thereby decreasing pH with acetic and pyruvic acidic metabolites in YUCG. Since the media did not contain acetic or pyruvic acids, the *pta-ack* pathway under glycerol and low nutrient conditions may account for this observed phenomenon (Grundy et al. 1993). Excessive carbohydrate in the form of glycerol might have led to extracellular acetic and pyruvic acids during growth through the acetyl-CoA-to-acetate pathway (Grundy et al. 1993). In verifying whether glucose supplement, which also supports better growth of strain JH7, leads to acidic pH and thus inhibits the MICP of strain JH7, pH changes were determined using bromothymol blue; the pH under the glucose-amended condition also became acidic (data not shown). Thus, it became clear that comparably high pH is crucial in engendering precipitates (Seifan et al. 2017).

Whenever bacteria encounter a new environment, it is inevitable for them to change their physiological characteristics to adapt to such atmospheric conditions. These characteristics could be membrane fluidity, EPS composition, cell elongation or contraction, and hydrophobicity (Ercole et al. 2007; Santana and Gonzalez 2015; Zhu and Dittrich 2016). Similarly, under different media conditions, the YUC and YUCG, strain JH7 induced dissimilar exopolysaccharide composition and amount, which may have altered the efficiency of capturing Ca^{2+}. Bacterial exopolysaccharides are affected by temperature and pH (Oggerin et al. 2013), and since the incubating temperature was constant throughout the assay (37 °C), the distinguishable exopolysaccharide composition in YUC and YUCG might be influenced by pH change, as the pH of YUCG media became relatively acidic at 72 h. Although the structure of exopolysaccharide extracted from YUCG media is not specifically determined as either heteropolysaccharide or homopolysaccharide or consisting of glucose, mannose, or arabinose, there is a possibility of the exopolysaccharide existing as a heteropolysaccharide, containing two or more different monosaccharide units. Repeating units of glucose and mannose can be

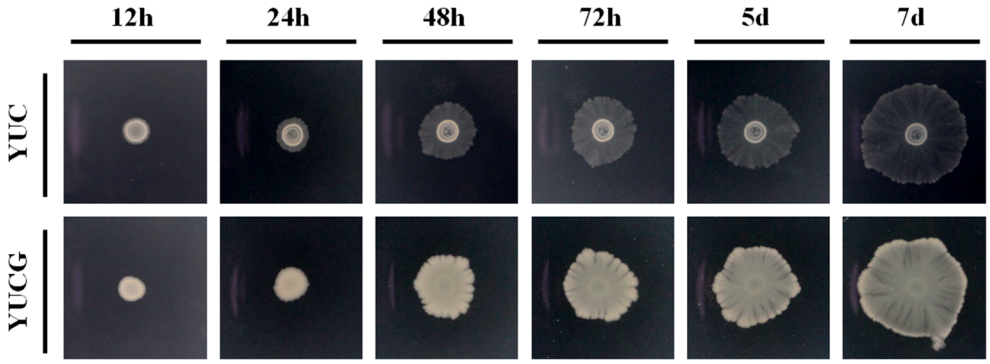

Fig. 6 Time-wise colony motility formation of strain JH7 inoculated in YUC and YUCG agar media

substituted by acetylated residues and pyruvate (Manca et al. 1996), which might favor capturing free Ca^{2+} ions, thereby reducing the chance of a MICP reaction in YUCG media. In fact, HPLC showed excessive amounts of acetic and pyruvic acid in YUCG, which may have decreased the concentration of mannose in the exopolysaccharide composition of YUCG. The results were consistent in ISE and qRT-PCR analysis, in that purified exopolysaccharide from YUCG had a higher efficiency in binding Ca^{2+}, and the amount of exopolysaccharide produced was distinctively higher, respectively (Fig. 4). In addition, the hydrophilic surface change of strain JH7 under glycerol might have increased the chance of supersaturation of Ca^{2+} on EPS. Hydrophilic surfaces can lead to higher cation binding capability since most hydrophilic functional groups of bacteria consist of mainly hydroxide (−OH) (Ercole et al. 2007; Baker et al. 2010; Renner and Weibel 2011), and these characteristics may increase resistance to hydrophobic circumstances such as non-charged minerals. Therefore, we speculated that the relatively hydrophilic strain JH7 incubated in YUCG was able to adhere to more Ca^{2+}, which decreased the chance of Ca^{2+} in participating in MICP (Fig. 5).

It is almost profound that cells inoculated in YUC and YUCG form different types of motility, as nutrients alter the general metabolism of signaling molecules related to production of microbial EPS and motility formation (Gallegos-Monterrosa et al. 2016). Both conditions had radial shaped motility, but with opacity distinction, probably due to growth differences and a differentiated regulation pattern of motility formation and EPS production of strain JH7. Although the wrinkle in YUC was thinner than YUCG, this may indicate higher demand of nutrients or water, thus forming a larger surface-volume ratio (Gallegos-Monterrosa et al. 2016) as YUC is relatively minimal and induces MICP. In fact, the encrustation of strain JH7 under YUC had a higher survival rate when exposed to 2 μg/ml of tetracycline, than strain JH7 incubated in LB (data not shown). Moreover, due to encrustation, it appeared that only a portion of cells was able to gain motility, as the opacity of circled belt remained similar over time.

This study is the first to analyze the inhibitory effect of excessive exopolysaccharide in the MICP of *Bacillus* sp. JH7 due to tight Ca^{2+} binding, owing to alteration of the chemistry changes in exopolysaccharide via glycerol. This study also provides insight into the mechanisms underlying bacterial MICP. The findings extend to the rational for bacterial calcium carbonate encrustation, as strain JH7 tends to precipitate calcium carbonate under a minimal nutrient state. Further extensive investigation on the functional mechanism of bacterial MICP is required; however, researchers should consider the interconnected roles of EPS in MICP for further application.

Acknowledgments This work was supported by a grant [16SCIP-B103706-02] from the Construction Technology Research Program funded by Ministry of Land, Infrastructure and Transport of the Korean government. This work is also supported by a Korea University grant (K1608401) to W. P.

Compliance with ethical standards This article does not contain any studies with human participants or animals performed by any of the authors.

Conflict of interest The authors declare that they have no conflict of interests.

References

Bai Y, Guo XJ, Li YZ, Huang T (2017) Experimental and visual research on the microbial induced carbonate precipitation by *Pseudomonas aeruginosa*. AMB Express 7:57. doi:10.1186/s13568-017-0358-5

Baker MG, Lalonde SV, Konhauser KO, Foght JM (2010) Role of extracellular polymeric substances in the surface chemical reactivity of *Hymenobacter aerophilus*, a psychrotolerant bacterium. Appl Environ Microbiol 76:102–109

Braissant O, Decho AW, Dupraz C, Glunk C, Przekop KM, Visscher PT (2007) Exopolymeric substances of sulfate-reducing bacteria: interactions with calcium at alkaline pH and implication for formation of carbonate minerals. Geobiology 5:401–411. doi:10.1111/j.1472-4669.2007.00117.x

Chowdhury SR, Basak RK, Sen R, Adhikari B (2011) Production of extracellular polysaccharide by *Bacillus megaterium* RB-05 using jute as substrate. Bioresour Technol 102:6629–6632

Couradeau E, Benzerara K, Gérard E, Moreira D, Bernard S, Brown GE Jr, López-García P (2012) An early-branching microbialite cyanobacterium forms intracellular carbonates. Science 336:459–462

De Muynck W, De Belie N, Verstraete W (2010) Microbial carbonate precipitation in construction materials: a review. Ecol Eng 36:118–136

De Philippis R, Colica G, Micheletti E (2011) Exopolysaccharide-producing cyanobacteria in heavy metal removal from water: molecular basis and practical applicability of the biosorption process. Appl Microbiol Biotechnol 92:697–708

Dupraz C, Reid RP, Braissant O, Decho AW, Norman RS, Visscher PT (2009) Processes of carbonate precipitation in modern microbial mats. Earth-Sci Rev 96:141–162

Ercole C, Cacchio P, Botta AL, Centi V, Lepidi A (2007) Bacterially induced mineralization of calcium carbonate: the role of exopolysaccharides and capsular polysaccharides. Microsc Microanal 13:42–50

Erşan YÇ, De Belie N, Boon N (2015) Microbially induced $CaCO_3$ precipitation through denitrification: an optimization study in minimal nutrient environment. Biochem Eng J 101:108–118

Gallegos-Monterrosa R, Mhatre E, Kovacs AT (2016) Specific *Bacillus subtilis* 168 variants do form biofilms on nutrient rich medium. Microbiology 162:1922–1932

Gat D, Ronen Z, Tsesarsky M (2016) Soil bacteria population dynamics following stimulation for ureolytic microbial-induced $CaCO_3$ precipitation. Environ Sci Technol 50:616–624

Grundy FJ, Waters DA, Allen SH, Henkin TM (1993) Regulation of the *Bacillus subtilis* acetate kinase gene by CcpA. J Bacteriol 175:7348–7355

Hammes F, Boon N, de Villiers J, Verstraete W, Siciliano SD (2003) Strain-specific ureolytic microbial calcium carbonate precipitation. Appl Environ Microbiol 69:4901–4909

Jansson C, Northen T (2010) Calcifying cyanobacteria—the potential of biomineralization for carbon capture and storage. Curr Opin Biotechnol 21:365–371

Jittawuttipoka T, Planchon M, Spalla O, Benzerara K, Guyot F, Cassier-Chauvat C, Chauvat F (2013) Multidisciplinary evidences that *Synechocystis* PCC6803 exopolysaccharides operate in cell

sedimentation and protection against salt and metal stresses. PLoS One 8:e55564

Kang CH, Han SH, Shin Y, Oh SJ, So JS (2014) Bioremediation of Cd by microbially induced calcite precipitation. Appl Biochem Biotechnol 172:2907–2915

Kim HJ, Eom HJ, Park C, Jung J, Shin B, Kim W, Chung N, Choi IG, Park W (2016) Calcium carbonate precipitation by *Bacillus* and *Sporosarcina* strains isolated from concrete and analysis of the bacterial community of concrete. J Microbiol Biotechnol 26:540–548

Kumar S, Shah AK (2015) Characterization of an adhesive molecule from *Bacillus megaterium* ADE-0-1. Carbohydr Polym 117:543–548

Kumari D, Qian XY, Pan X, Achal V, Li Q, Gadd GM (2016) Microbially-induced carbonate precipitation for immobilization of toxic metals. Adv Appl Microbiol 94:79–108

Manca MC, Lama L, Improta R, Esposito E, Gambacorta A, Nicolaus B (1996) Chemical composition of two exopolysaccharides from *Bacillus thermoantarcticus*. Appl Environ Microbiol 62:3265–3269

Nwodo UU, Green E, Okoh AI (2012) Bacterial exopolysaccharides: functionality and prospects. Int J Mol Sci 13:14002–14015

Oggerin M, Tornos F, Rodríguez N, del Moral C, Sánchez-Román M, Amils R (2013) Specific jarosite biomineralization by *Purpureocillium lilacinum*, an acidophilic fungi isolated from Rio Tinto. Environ Microbiol 15:2228–2237

Park JM, Park SJ, Ghim SY (2013) Characterization of three antifungal calcite-forming bacteria, *Arthrobacter nicotianae* KNUC2100, *Bacillus thuringiensis* KNUC2103, and *Stenotrophomonas maltophilia* KNUC2106, derived from the Korean islands, Dokdo and their application on mortar. J Microbiol Biotechnol 23:1269–1278

Park H, Park B, Kim HJ, Park W, Choi IG (2016) Draft genome sequences of two ureolytic bacteria isolated from concrete block waste. Genome Announc 4:e00762–e00716. doi:10.1128/genomeA.00762-16

Peighamy-Ashnaei S, Sharifi-Tehrani A, Ahmadzadeh M, Behboudi K (2007) Effect of carbon and nitrogen sources on growth and biological efficacy of *Pseudomonas fluorescens* and *Bacillus subtilis* against *Rhizoctonia solani*, the causal agent of bean damping-off. Commun Agric Appl Biol Sci 72:951–956

Pereira S, Zille A, Micheletti E, Moradas-Ferreira P, De Philippis R, Tamagnini P (2009) Complexity of cyanobacterial exopolysaccharides: composition, structures, inducing factors and putative genes involved in their biosynthesis and assembly. FEMS Microbiol Rev 33:917–941

Renner LD, Weibel DB (2011) Physiochemical regulation of motility formation. MRS Bull 36:347–355. doi:10.1557/mrs.2011.65

Rusznyák A, Akob DM, Nietzsche S, Eusterhues K, Totsche KU, Neu TR, Frosch T, Popp J, Keiner R, Geletneky J, Katzschmann L, Schulze ED, Küsel K (2012) Calcite biomineralization by bacterial isolates from the recently discovered pristine karstic herrenber cave. Appl Environ Microbiol 78:1157–1167

Santana MM, Gonzalez JM (2015) High temperature microbial activity in upper soil layers. FEMS Microb Lett 362:fnv182. doi:10.1093/femsle/fnv182

Seifan M, Samani AK, Berenjian A (2016) Induced calcium carbonate precipitation using *Bacillus* species. Appl Microbiol Biotechnol 100:9895–9906

Seifan M, Samani AK, Berenjian A (2017) New insights into the role of pH and aeration in the bacterial production of calcium carbonate ($CaCO_3$). Appl Microbiol Biotechnol 101:3131–3142

Shao PP, Comolli LR, Bernier-Latmani R (2014) Membrane vesicles as a novel strategy for shedding encrusted cell surfaces. Fortschr Mineral 4:74–88. doi:10.3390/min4010074

Tourney J, Ngwenya BT, Fred Mosselmans JW, Magennis M (2009) Physical and chemical effects of extracellular polymers (EPS) on Zn adsorption to *Bacillus licheniformis* S-86. J Colloid Interface Sci 15:381–389

Zamarreño DV, Inkpen R, May E (2009) Carbonate crystals precipitated by freshwater bacteria and their use as a limestone consolidant. Appl Environ Microbiol 75:5981–5990

Zhu T, Dittrich M (2016) Carbonate precipitation through microbial activities in natural environment, and their potential in biotechnology: a review. Front Bioeng Biotechnol 4:4. doi:10.3389/fbioe.2016.00004

Zivkovic M, Miljkovic M, Ruas-Madiedo P, Strahinic I, Tolinacki M, Golic N, Kojic M (2015) Exopolysaccharide production and ropy phenotype are determined by two gene clusters in putative probiotic strain *Lactobacillus paraplantarum* BGCG11. Appl Environ Microbiol 81:1387–1396